Observation of Strong Ordering in $Ga_x In_{1-x} P$ Alloy Semiconductors

Akiko Gomyo and Tohru Suzuki

Opto-Electronics Research Laboratories, NEC Corporation, Miyamae-ku, Kawasaki 213, Japan

and

Sumio Iijima

Fundamental Research Laboratories, NEC Corporation, Miyamae-ku, Kawasaki 213, Japan
(Received 15 October 1987)

Extremely strong superstructure reflections have been observed for the first time by transmission electron microscopy for (110) edge-on $Ga_{0.5}In_{0.5}P$ crystals lattice matched to GaAs. Growth was carried out by metal-organic vapor-phase epitaxy. A monolayer superlattice (SL) of (Ga-rich plane) (In-rich plane) ... is formed along $[\bar{1}11]$ and $[1\bar{1}1]$ directions. The substrates are found to be playing a vital role in the SL formation. Band-gap energy reduction ($\simeq 80$ meV) has been observed for layers with these SL's.

The recent observation of long-range order (LRO) of Al and Ga on column-III sublattice in the $Al_xGa_{1-x}As$ alloy semiconductor[1] is quite important in regard to thermodynamics for III-V alloy semiconductors. LRO has also been found in other III-V alloys, such as $Ga_xIn_{1-x}As$,[2-4] $GaAs_xSb_{1-x}$,[5] and $Ga_xIn_{1-x}P_yAs_{1-y}$.[4] Independently from the first observation for $Al_xGa_{x-1}As$, Srivastava, Martins, and Zunger have predicted atomic ordering in alloy semiconductors, taking $Ga_xIn_{1-x}P$ as an illustrative example.[6]

In a previous paper,[7] we have reported $\mp \frac{1}{2}, \pm \frac{1}{2}, 0$ electron-beam superstructure reflection spots, whose intensities were very weak, for $Ga_{0.5}In_{0.5}P$ crystals and proposed a bilayer superlattice (SL) on $(\bar{1}10)$ planes for Ga and In arrangements, based only on $[001]^*$ zone-axis electron-diffraction studies.

In this Letter, intense superstructure reflections from (110) edge-on $Ga_{0.5}In_{0.5}P$ crystals lattice matched to GaAs are reported. A Ga and In monolayer SL formed in a $[\bar{1}11]$ direction is found to be a dominant LRO. Substrate orientation effects on the SL formation are presented and discussed. The band-gap energy of $Ga_{0.5}In_{0.5}P$ with the LRO has been found to be about 80 meV lower in value than that for crystals with no LRO. The interpretation[7] for the previously reported weak $\mp \frac{1}{2}, \pm \frac{1}{2}, 0$ reflections is reexamined.

Undoped $\simeq 0.5$-μm-thick $Ga_{0.5}In_{0.5}P$ crystals were grown by metal-organic vapor-phase epitaxy under several growth temperatures (T_g).[8] V/III ratios[8] were $\simeq 400$, unless mentioned. A zinc-doped crystal was also studied. The epitaxial layers were lattice matched to (001) 2° off to [011] GaAs, unless specially mentioned. The degree of lattice matching was examined by a double-crystal x-ray diffractometer. Samples for transmission electron microscopy were prepared by mechanical polishing and Ar-ion etching for $[110]^*$ and $[\bar{1}10]^*$ zone-axis observations. Chemical etching was employed for $[001]^*$ zone-axis observations. Figure 1(a) shows a typical $[110]^*$ zone-axis transmission electron-diffraction (TED) pattern for an undoped $Ga_{0.5}In_{0.5}P$ crystal grown under a condition of $T_g = 700$ °C. Extremely strong superstructure reflection spots ($-\frac{1}{2}, \frac{1}{2}, \frac{1}{2}; ...$) are observed halfway between the rows of basic matrix spots ($\bar{1}11; ...$). Similar but relatively weak spots ($\frac{1}{2}, -\frac{1}{2}, \frac{1}{2}; ...$) are present along $[1\bar{1}1]$. Two sets of weak spots $0, 0, \pm 1$ and $\mp 1, \pm 1, 0$ can be attributed to double reflections. A $[\bar{1}10]^*$ zone-axis TED pattern did not show superstructure reflection spots. The strong superstructure reflection spots seen in Fig. 1(a), together with the result for the $[\bar{1}10]^*$ zone-axis observation just mentioned, indicate that a monolayer SL of a sequence of (Ga-rich plane)(In-rich plane)(Ga-rich plane)(In-rich plane)... in the $[\bar{1}11]$ direction is a main feature of the atom arrangement on the column-III sublattice.

The appearances of the TED pattern have been found to depend on the metal-organic vapor-phase epitaxy growth conditions. At 750 °C, the superstructure reflections remain spotty in their shape, similar to that shown in Fig. 1(a). The superstructure reflection spots in Fig. 1(a) are accompanied by streaks nearly parallel to the $[001]^*$ growth axis. The appearance of the streaks is rather complex. The streak lines stem from rational fraction points $\mp \frac{1}{2}, \pm \frac{1}{2}, \frac{1}{2}$ an an angle of $\simeq 10°$ for a small distance and then extend continuously in $[001]^*$ directions. The complex appearance is much more clearly observed for samples with lower T_g values. The elongation of the 10° angle streaks from the $\mp \frac{1}{2}, \pm \frac{1}{2}, \frac{1}{2}$ positions becomes greater for samples with lower T_g ($\lesssim 600$ °C). All the features of the streaks become wavy and diffusive, as shown in Figs. 1(b) and 1(c). The 600 °C case [Fig. 1(b)] does not show sharp spots at $\mp \frac{1}{2}, \pm \frac{1}{2}, \frac{1}{2}$ positions [e.g., point p in Fig. 1(b)]. Instead, diffuse scattering is observed. Point p' in Fig. 1(b) is a position $-(\frac{1}{2} - \delta), \frac{1}{2} - \delta, 0$, where the
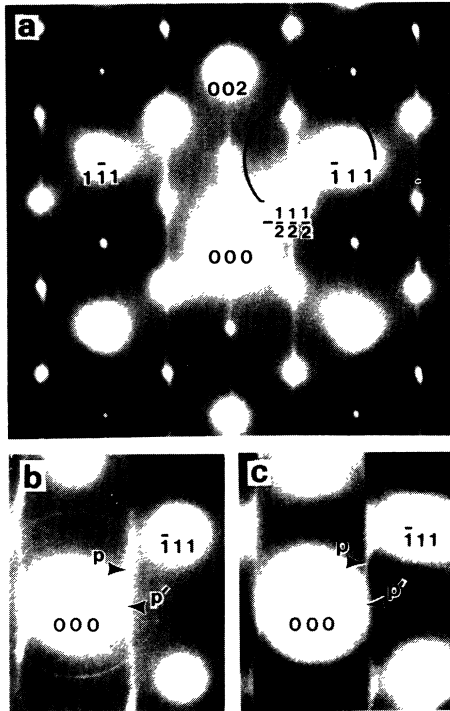
FIG. 1. $[110]^*$ zone-axis electron-diffraction patterns for three growth temperatures. (a) A TED pattern from a $Ga_{0.5}In_{0.5}P$ crystal showing strong superstructure spots $(-\frac{1}{2},\frac{1}{2},\frac{1}{2};...)$ along the $[\bar{1}11]^*$ direction but weak spots along $[1\bar{1}1]^*$. The crystal was grown at $T_g = 700\,°C$. The meaning of the black circle is given in the caption for Fig. 2. (b) A TED pattern for a sample grown at $T_g = 600\,°C$. (c) A TED pattern for a sample grown at $T_g = 550\,°C$. The $\approx 10°$ inclination to the $\pm[001]^*$ directions at the $-\frac{1}{2},\frac{1}{2},\frac{1}{2}$ and $-\frac{1}{2},\frac{1}{2},\frac{3}{2}$ positions and wavy features of the streaks are clearly observed in (b) and (c). p and p', indicated by arrows, show the positions of $-\frac{1}{2},\frac{1}{2},\frac{1}{2}$, and $-(\frac{1}{2}-\delta),\frac{1}{2}-\delta,0$, respectively, where the values of δ are given in the text.
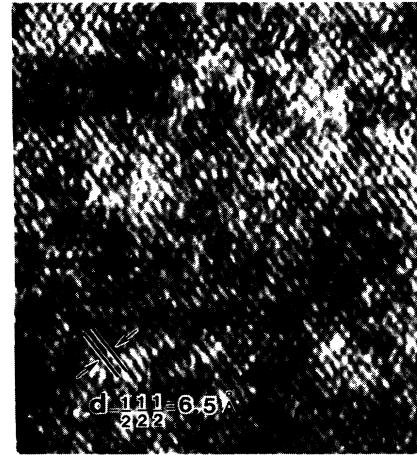

FIG. 2. A dark-field electron micrograph taken from the same crystal as that of Fig. 1(a) which was recorded by use of the three spots encircled in Fig. 1. Dominance of the $(-\frac{1}{2},\frac{1}{2},\frac{1}{2})$ superstructure lattice images can be seen. There are some disorder regions (top left).

streak intersects the $[001]^*$ zone-axis Ewald sphere. The δ value is small and positive, around 0.03. At $550\,°C$ the diffuse-scattering maximum moves to the position $-(\frac{1}{2}-\delta),\frac{1}{2}-\delta,0$ [p' in Fig. 1(c)], where δ is ≈ 0.05. The δ value at $700\,°C$ is very small, but still positive $(0 < \delta < 0.004)$. It is noticed that the exact coordinates of the previously reported[7] $\mp\frac{1}{2},\pm\frac{1}{2},0$ superstructure spots in the $[001]^*$ zone-axis TED pattern[7] are $\mp(\frac{1}{2}-\delta'),\pm(\frac{1}{2}-\delta'),0$, where δ' is a small positive value. The δ' values are found to agree well with the deviations δ for samples grown at various T_g and V/III values. TED patterns in the $[001]^*$ zone axis were also studied, by our tilting a sample $(T_g = 600\,°C)$ from $[001]$ towards $\pm[\bar{1}10]$ directions up to $10°$. The positions of the superstructure spots in the $[001]^*$ zone axis were actually found to be the intersections of the Ewald sphere with the wavy streaks seen in the $[110]^*$ zone-axis TED pattern [Fig. 1(b)]. Thus, the superstructure spots in the

$[110]^*$ zone axis, which were previously expected to be due to LRO,[7] should be interpreted as the intersections of the three-dimensional wavy-streak rods.

A dark-field electron micrograph (Fig. 2) was recorded from the same crystal as that for Fig. 1(a) by use of three reflection spots: $\bar{1},1,1$, $-\frac{1}{2},\frac{1}{2},\frac{1}{2}$, and $-\frac{1}{2},\frac{1}{2},\frac{3}{2}$. The latter two reflection spots are due to the superstructures. The $(-\frac{1}{2},\frac{1}{2},\frac{1}{2})$ superstructure lattice images (spacing $= 6.5$ Å), which run from the top left to the bottom right, appear predominantly over the $(-\frac{1}{2},\frac{1}{2},\frac{3}{2})$ lattice images which appear in smaller regions. Dark-field images for samples with lower T_g suggest that the above-mentioned wavy and diffuse reflections can be ascribed to many (001) antiphase boundaries (APB's) which occur at intervals of several atomic layers in the [001] growth direction. A statistical variation of these small intervals in the [001] direction for (001) APB's will give rise to the diffuse scattering. However, waviness of the diffuse scattering cannot be explained simply by a series of APB's in the [001] direction. The above-mentioned positive deviation δ, which represents "waviness" of streaks, means a small local lattice expansion by a ratio $1 + 2\delta$ in the $[\bar{1}10]$ direction due to a strain field around the APB's. As T_g lowers from $700\,°C$, the number of APB's increases, and, at the same time, the δ value increases. This means that the increased number of APB's results in a larger lattice distortion (larger δ) around the APB's. The origin of the wavy and diffuse nature of the streaks, however, deserves separate and further studies and will be published later.

For TED intensities, the intensity at a $-\frac{1}{2},\frac{1}{2},\frac{1}{2}$ position shows a maximum intensity for a T_g range from 650 to $700\,°C$ [Fig. 1(a)] at V/III ≈ 400 and shows weaker intensities at higher or lower temperatures. When T_g

lowers from 700 °C, the integral intensity for the diffuse reflections, other than the basic matrix reflection spots $(\bar{1},1,1;0,0,2;\ldots)$, also becomes weaker, as well as the intensity at a $-\frac{1}{2},\frac{1}{2},\frac{1}{2}$ position [Figs. 1(b) and 1(c)]. Note the relative intensities between these reflections and the basic matrix spots, e.g., the $\bar{1},1,1$ spot. The intensity of the superstructure reflection for the 750 °C case is much weaker than that for the 700 °C case. The decrease in superstructure reflection intensity at a higher temperature ($\simeq 750$ °C) may be due to random mixing of Ga and In on the growth surface by entropy effect.[1] The decrease in the intensity at a lower temperature ($\simeq 550$ °C) may be due to a decrease in surface mobilities[1] of Ga and In atoms on the growth surface and the resultant APB increase and random configuration dominance.

There are four equivalent $\langle\bar{1}11\rangle$ directions: $[\bar{1}11]$, $[1\bar{1}1]$, $[11\bar{1}]$, and $[\bar{1}\bar{1}\bar{1}]$. If the monolayer SL formation were only the consequence of the $Ga_{0.5}In_{0.5}P$ bulk crystal's thermodynamic properties, SL's along the $[11\bar{1}]$ and $[\bar{1}\bar{1}1]$ directions should also be observed, as well as along the $[\bar{1}11]$ and $[1\bar{1}1]$ directions. Here, "bulk crystal" means a crystal without a boundary. This is, however, not the case; i.e., we have never observed the $[11\bar{1}]$ and $[\bar{1}\bar{1}1]$ variants. The cause of this asymmetry in the appearance of the four equivalent SL variants should therefore be ascribed to a boundary effect; the symmetry is being broken by the existence of a boundary, i.e., a GaAs substrate. There is asymmetry for As-atom dangling-bond directions on an As-stabilized (001) GaAs surface. The directions of the projected dangling bonds to the (001) surface are $\pm[\bar{1}10]$, and not $\pm[110]$. This asymmetry at the boundary, i.e., on the substrate surface, is considered to make the appearance of SL variants asymmetric.

In an attempt to investigate the cause of the superstructure intensity asymmetry (seen in Fig. 1) for the $[\bar{1}11]$- and $[1\bar{1}1]$-direction SL's, we have examined $Ga_{0.5}In_{0.5}P$ layers grown on (001) 2° off to [110] GaAs (sample A) and (001) 2° off to $[\bar{1}10]$ GaAs (sample B). Both layers showed the $[\bar{1}11]^*$- and $[1\bar{1}1]^*$-direction superstructures. An intensity asymmetry similar to that seen in Fig. 1 was also observed for sample B. The intensities for the two superstructure reflection spots from sample A, however, were approximately the same. The substrate-surface inclination component from the [001] to the $[\bar{1}10]$ direction is thus responsible for the observed dominance (Fig. 1) of the $[\bar{1}11]$-direction SL. From these observations, an array of atomic steps, descending to the $[\bar{1}10]$ direction on the GaAs surface, will be working so as to break the superstructure formation symmetry. Though sample A has no macroscopic inclination to the $[\bar{1}10]$ direction, it should have, microscopically, an approximately equal number of descending and ascending atomic-scale steps to the $[\bar{1}10]$ direction. These steps probably give rise to the equal appearance of both SL's in sample A. Further studies on the cause of the natural superlattice formation are under way.

The SL observed in the present study does not coincide with any of the theoretically predicted superstructures.[6,9] The $[110]^*$ zone-axis TED patterns are rather similar to that for vapor-phase-epitaxially grown $Ga_xIn_{1-x}As$, reported very recently.[4] The monolayer SL in the $[\bar{1}11]$ direction in $Ga_{0.5}In_{0.5}P$ is identical to that in $Ga_xIn_{1-x}As$. Shahid, Mahajan, and Laughlin observed one variant: $[\bar{1}11]$ SL for $Ga_{0.5}In_{0.5}As$ on (001) InP.[10] We have, however, observed two variants. From the present study, their observation can be interpreted in such a way that their (001) InP substrate surface might be a vicinal face having an inclination component toward $[\bar{1}10]$, although there is no explicit description about it, and that they failed to observe the other variant $[1\bar{1}1]$ because this second variant should be too weak to be observed because of the expected large intensity asymmetry between the two variants. However, as for the superstructure reflection intensity, the present case shows several orders of magnitude stronger reflection intensity than that for $Ga_{0.5}In_{0.5}As$. The experimentally observed much

TABLE I. Band-gap energies and electron-beam reflection intensities at the $-\frac{1}{2},\frac{1}{2},\frac{1}{2}$ position observed for $Ga_{0.5}In_{0.5}P$ grown on GaAs by metal-organic vapor-phase epitaxy under various growth conditions.

Sample	Growth conditions T_g (°C)	V/III	Doping	E_g [a] (eV, 300 K)	Electron-beam reflection intensity at $-\frac{1}{2},\frac{1}{2},\frac{1}{2}$
S1	550	455	Undoped	1.902	Very weak
S2	600	421	Undoped	1.871	Weak
S3	650	222	Undoped	1.83	Strong
S4	700	62	Undoped	1.894	Weak
S5	700	130	Zn doped[b]	1.914	None
S6	700	405	Undoped	1.835	Strong
S7	750	421	Undoped	1.883	Weak

[a] E_g was determined with photoluminescence.
[b] $[p] \simeq 1 \times 10^{18}$ cm^{-3}.

stronger intensity for $Ga_{0.5}In_{0.5}P$ than that for $Ga_{0.5}In_{0.5}As$ is concluded to be mainly due to the higher degree of ordering in $Ga_{0.5}In_{0.5}P$, based on dynamical structure-factor calculations.

The band-gap energy (E_g) of $Ga_{0.5}In_{0.5}P$ lattice matched to GaAs is dependent on T_g [7,8,11] and the V/III ratio.[7,8] Table I shows the E_g value and reflection intensity at $-\frac{1}{2}, \frac{1}{2}, \frac{1}{2}$ in the reciprocal-lattice coordinate for samples grown under various growth conditions. The hitherto reported $E_g(300$ K) values for liquid-phase-epitaxy $Ga_{0.5}In_{0.5}P$ are concentrated around 1.9 eV.[12] There is a tendency for the E_g value to decrease with increasing reflection intensity. The minimum E_g value observed in the present study was $\simeq 20$ meV lower than that mentioned in the previous report,[7] which may be because of a slightly higher degree of ordering caused by a small deviation in the growth condition from growth to growth. Samples with "anomalously" low E_g (1.83–1.85 eV) show very strong superstructure spot intensity, indicating that the electron energy-band structure having the SL is different from that with random distribution of Ga and In on the sublattice. Sample S5 is a highly zinc-doped $([p] \simeq 1 \times 10^{18}$ cm$^{-3})$ $Ga_{0.5}In_{0.5}P$. No superstructure spot can be observed for S5, and E_g takes a high value of $\simeq 1.914$ eV. This result can be explained as follows: The SL on the column-III sublattice is destroyed and not formed during growth with high zinc doping. This phenomenon seems very similar to the previously reported zinc-diffusion effect,[7] which also makes an anomalously low E_g value higher.

$Ga_{0.5}In_{0.5}P$ is used for a light-emitting layer ("active layer") of AlGaInP visible semiconductor lasers.[13] The $\simeq 80$-meV band-gap energy difference is directly related to the difference in lasing wavelength, which severely (by an order of magnitude) influences visibility of the laser light in the wavelength region ($\simeq 670$ nm). The SL formation in $Ga_{0.5}In_{0.5}P$ and the observed band-gap energy reduction are thus important, from a practical point of view, as well as from a scientific aspect.

The authors would like to thank K. Kobayashi, S. Kawata, H. Fujii, H. Hotta, I. Hino, and T. Yuasa for growing crystals and helpful discussions. The authors also would like to thank T. Kawamura and H. Kitajima for helpful discussions.

Note added.—After the submission of the original manuscript, two other papers were published.[14] These two articles have also reported $\langle 111 \rangle$ SL's in $Ga_{0.5}In_{0.5}P$ and $GaAs_{0.5}Sb_{0.5}$, respectively. It is noticed that the appearance asymmetry of the SL reported by Ueda et al. is different from that in the present paper. We have consistently observed the intensity asymmetry similar to that reported by Ueda et al. only in crystals grown on (001) GaAs with a misorientation component towards the [1$\bar{1}$0] direction ($-$[$\bar{1}$10]), as was described in the present text.

[1]T. S. Kuan, T. F. Kuech, W. I. Wang, and E. L. Wilkie, Phys. Rev. Lett. **54**, 201 (1985).

[2]H. Nakayama and H. Fujita, in *Gallium Arsenide and Related Compounds—1985*, edited by M. Fujimoto, IOP Conference Proceedings No. 79 (Hilger, Boston, 1986), p. 289.

[3]T. S. Kuan, W. I. Wang, and L. Wilkie, Appl. Phys. Lett. **51**, 51 (1987).

[4]M. A. Shahid, S. Mahajan, and D. E. Laughlin, Phys. Rev. Lett. **58**, 2567 (1987).

[5]H. R. Jen, M. J. Cherng, and G. B. Stringfellow, Appl. Phys. Lett. **48**, 1603 (1986).

[6]G. P. Srivastava, J. L. Martins, and A. Zunger, Phys. Rev. B **31**, 2561 (1985).

[7]A. Gomyo, T. Suzuki, K. Kobayashi, S. Kawata, I. Hino, and T. Yuasa, Appl. Phys. Lett. **50**, 673 (1987). In this paper, the [110] and [$\bar{1}$10] directions should be reversed in order to be consistent with the present notation.

[8]A. Gomyo, K. Kobayashi, S. Kawata, I. Hino, T. Suzuki, and T. Yuasa, J. Cryst. Growth **77**, 367 (1986). V/III stands for a source-gas flow-rate ratio, i.e., a ratio of column-V source-gas flow rate to a sum of column-III source-gas flow rates.

[9]A. A. Mbaye, L. G. Ferreira, and A. Zunger, Phys. Rev. Lett. **58**, 49 (1987).

[10]The notation [110] used in Ref. 4 corresponds to our [$\bar{1}$10].

[11]Y. Oba, M. Ishikawa, H. Sugawara, M. Yamamoto, and T. Nakanishi, J. Cryst. Growth **77**, 374 (1986).

[12]H. Asai and K. Oe, J. Appl. Phys. **53**, 6849 (1982).

[13]T. Suzuki, *Extended Abstracts of the Eighteenth International Conference on Solid State Devices and Materials, Tokyo, 1986* (Business Center for Academic Societies, Tokyo, Japan, 1986), p. 149.

[14]O. Ueda, M. Takikawa, J. Komeno, and J. Umebu, Jpn. J. Appl. Phys. **26**, L1824 (1987); Y. E. Ihm, N. Otsuka, J. Klem, and H. Morkoç, Appl. Phys. Lett. **51**, 2013 (1987).

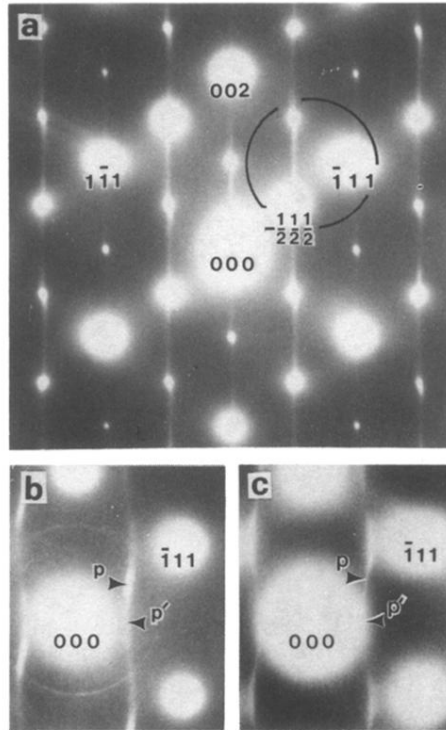FIG. 1. [110]* zone-axis electron-diffraction patterns for three growth temperatures. (a) A TED pattern from a $Ga_{0.5}In_{0.5}P$ crystal showing strong superstructure spots $(-\frac{1}{2}, \frac{1}{2}, \frac{1}{2}; \ldots)$ along the $[\bar{1}11]^*$ direction but weak spots along $[1\bar{1}1]^*$. The crystal was grown at $T_g = 700\,°C$. The meaning of the black circle is given in the caption for Fig. 2. (b) A TED pattern for a sample grown at $T_g = 600\,°C$. (c) A TED pattern for a sample grown at $T_g = 550\,°C$. The $\simeq 10°$ inclination to the $\pm[001]^*$ directions at the $-\frac{1}{2}, \frac{1}{2}, \frac{1}{2}$ and $-\frac{1}{2}, \frac{1}{2}, \frac{3}{2}$ positions and wavy features of the streaks are clearly observed in (b) and (c). p and p', indicated by arrows, show the positions of $-\frac{1}{2}, \frac{1}{2}, \frac{1}{2}$, and $-(\frac{1}{2} - \delta), \frac{1}{2} - \delta, 0$, respectively, where the values of δ are given in the text.
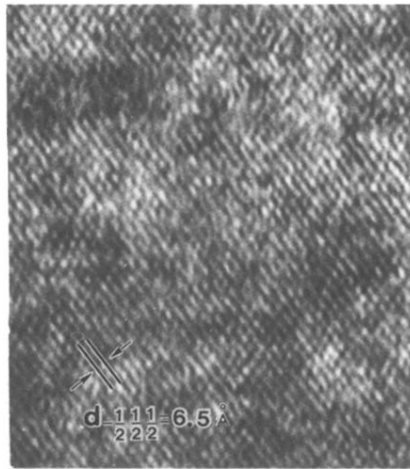
FIG. 2. A dark-field electron micrograph taken from the same crystal as that of Fig. 1(a) which was recorded by use of the three spots encircled in Fig. 1. Dominance of the $(-\frac{1}{2}, \frac{1}{2}, \frac{1}{2})$ superstructure lattice images can be seen. There are some disorder regions (top left).